J Comp Physiol A (1992) 170:227–241

Journal of Comparative Physiology A Sensory, Neural, and Behavioral Physiology

Discharge patterns of cochlear ganglion neurons in the chicken

R.J. Salvi,* S.S. Saunders, N.L. Powers, and F.A. Boettcher

Hearing Research Laboratory, Department of Communication Disorders & Sciences, State University of New York at Buffalo, 215 Parker Hall, Buffalo, New York 14214, USA

Accepted November 21, 1991

Summary. Physiological recordings were made of the compound action potential from the round window and single neurons in the cochlear ganglion of normal adult chickens *(Gallus domesticus)*. The compound action potential threshold to tone bursts decreased from approximately 42 dB at 0.25 kHz to 30 dB between 1 and 2 kHz and then increased to 51 dB at 4 kHz. Most of the cochlear ganglion cells had characteristic frequencies below 2 kHz and the thresholds of most neurons were roughly 30–35 dB lower than the compound action potential thresholds. At any given characteristic frequency, thresholds varied by as much as 60 dB and units with the highest thresholds tended to have the lowest spontaneous rates. Spontaneous discharge rates ranged from 0 to 200 spikes/s with a mean rate of 86 spikes/s. Interspike interval histograms of spontaneous activity often contained regular peaks with the time interval between peaks approximately equal to 1/(characteristic frequency). Tuning curves were sharply tuned and V-shaped with approximately equal slopes to the curves above and below characteristic frequency. Q_{10dB} and Q_{30dB} values for the tuning curves increased with characteristic frequency. Post stimulus time histograms showed sustained firing during the stimulus and were characterized by a slight-to-moderate peak at stimulus onset. Most units showed vigorous phase-locking to tones at characteristic frequency although the degree of phase-locking declined sharply with increasing characteristic frequency. Discharge rate-level functions at characteristic frequency had a mean dynamic range of 42 dB and a mean saturation firing rate of 327 spikes/s. In general, the firing patterns of cochlear ganglion neurons are similar in most respects to those reported in other avians, but differ in several important respects from those seen in mammals.

Key words: Cochlear ganglion neurons – Characteristic frequency – Threshold – Tuning curve – Spontaneous activity

Introduction

The chicken *(Gallus domesticus)* is a widely available species, and in recent years it has become a popular animal in hearing research (Saunders and Tilney 1982; Corwin and Cotanche 1988; Rubel et al. 1984; Manley et al. 1987). The audiogram of the chicken has been established and several other of its auditory processing abilities have been measured behaviorally (Gray 1990; Gray and Rubel 1985a, b). Progress has also been made in describing the anatomy of the peripheral and central auditory system of adult and developing animals (Tilney et al. 1987; Fermin and Cohen 1984; Jhavari, and Morest 1982; Rubel and Parks 1975) and neurophysiological measurements have been obtained from different regions of the auditory pathway. Auditory evoked potentials recorded from the cochlea and auditory brainstem have provided insights on the sensitivity and frequency selectivity of the system (Saunders et al. 1973; McFadden and Saunders 1989) and microelectrodes have been used to characterize the response properties of hair cells (Patuzzi and Bull 1991; Fuchs et al. 1988) and single neurons in nucleus magnocellularis and nucleus angularis (Warchol and Dallos 1990). Recordings have also been obtained from cochlear ganglion neurons in chicks in order to evaluate the tonotopic organization of the basilar papilla as a function of age (Manley et al. 1987); however, a detailed description of the response properties of spiral ganglion neurons is, to our knowledge, not yet available. Such information is essential for understanding the transformations in the neural code that take place between the hair cells and auditory nerve and between the auditory nerve and more central auditory nuclei. In addition, this information could prove useful in comparing

Abbreviations: *CF* characteristic frequency; *CAP* compound action potential

* To whom reprint requests should be sent

the discharge patterns of cochlear ganglion neurons in the chicken with those from other avian ears or those from mammals. Finally, hair cell regeneration has been shown to occur in chickens as well as other avian ears (Corwin and Cotanche 1988; Ryals and Rubel 1987); however, it is not yet known if the functional characteristics of cochlear ganglion neurons which synapse on regenerated hair cells regain their normal functional characteristics. In order to evaluate this issue in the chicken, it is necessary to have baseline measures of normal function for comparison. Thus, the purpose of the present study was to provide a relatively comprehensive description of the normal discharge patterns of cochlear ganglion neurons in the adult chicken.

Methods

The surgical procedures for recording from cochlear ganglion neurons in chickens are similar to those described by Manley et al. (1985). Briefly, white Leghorn chickens *(Gallus domesticus)* weighing between 0.8–1.5 kg were initially anesthetized by an intramuscular injection of ketamine (80–100 mg/kg) and xylazine (2–4 mg/kg) and then maintained in this state with supplemental doses of sodium pentobarbital (65 mg/kg) as needed. Body temperature was maintained at 41 °C using a heating pad coupled to a thermocouple inserted into the pectoralis muscle. During the experiment, the animals were given subcutaneous injections of bird Ringer's solution at intervals of approximately 1.5 h. In the initial experiments, the animals were not artificially ventilated; however, it was often difficult to obtain stable recordings under these conditions. Therefore, in later experiments the animals were tracheotomized and unidirectionally ventilated (1.3–1.8 l/m) with humidified air after making a hole in an abdominal air sac. The skin and muscle on the dorsal surface of the skull were removed and a metal rod was attached to the skull using small screws and dental cement. The rod was then mounted to a small clamp on a magnetic base in order to stabilize the head during the recordings. The middle ear space was opened by removing the bone overlying the postero-lateral surface of the skull thereby allowing the round window membrane and basal region of the basilar papilla to be visualized. A silver ball electrode was placed near the round window and cemented into place. Then the inner ear was opened in the region of recessus scala tympani to expose the cochlear ganglion, which appeared as a white band deep within scala tympani. A sound source (B&K 4134 microphone driven in reverse) and probe tube microphone (Etymotics ER-7C) assembly was sealed into the ear canal. The sound source was calibrated between 100 Hz and 10 kHz under computer control and the calibration values were stored on disk for later use.

Recordings were carried out in an electrically shielded, double-walled sound booth. The compound action potential (CAP) was recorded from the round window electrode. The output of the electrode was amplified (10,000 ×), filtered (0.1–10 kHz), and then digitized (25 kHz sampling rate, 256 points) by the A/D converter (16 bits) on a signal processing board (Spectrum Signal Processing TMS320C25) located in a personal computer. The CAP was elicited with tone bursts (5 ms duration, 1 ms rise/fall, cosine gating, 10/s). All stimuli were generated digitally (50 kHz sampling rate) using a signal processing board with D/A converter (Spectrum Signal Processing, TMS320C25) followed by a low pass (TDK HFL0030) filter with a roll off of 90 dB between 20 and 24 kHz.

Action potentials from spiral ganglion neurons were recorded with glass micropipettes (3 *M* potassium acetate, 20–50 MΩ). The electrode was advanced by an hydraulic microdrive (Trent Wells) in one micron steps while search stimuli (swept frequency tone bursts) were presented. The output of the electrode was amplified (variable gain), filtered (0.1–3 kHz), and then delivered in parallel to an oscilloscope, audio monitor and A/D converter on a signal processing board in a computer (Spectrum Signal Processing TMS320C25). The spike discharges were digitized and displayed on the monitor of the computer along with the spike trigger level. Spike arrival times relative to stimulus onset were measured with a resolution of 20 μs and stored on disk for later analysis. Spontaneous discharge rate was sampled for 10–20 s. Tuning curves were measured using a computer automated threshold tracking procedure which uses a threshold criterion based on a 1 spike difference between the number of discharges that occur in the tone interval (50 ms, 1 ms rise/fall, cosine gating) and no-tone interval (50 ms) (Liberman 1978; Salvi et al. 1982). Tuning curves were typically measured with a resolution of 32 points per octave. Tone bursts (50 ms, 1 ms rise/fall, cosine gating) were presented at the unit's characteristic frequency (CF) at levels ranging from −10 dB to 70 dB re threshold and the measurements were used to construct discharge-rate level functions, post-stimulus time histograms and period histograms.

Results

Compound action potential

Figure 1 shows a series of CAP waveforms collected at 0.25, 0.5, 1 and 2 kHz. At low sound levels, the waveforms consisted primarily of a negative peak (N_1) followed by a positive peak (P_1). The latency of the N_1 component of the CAP systematically decreased from approximately 2.5–3 ms near threshold to approximately 1.2–1.3 ms at 95 dB SPL. At high stimulus levels, very large amplitude oscillations were present in the response to 0.5 and 1 kHz tone bursts. The frequency of the oscillations was roughly twice the stimulus frequency. These oscillations could conceivably be due to incomplete cancellation of the cochlear microphonics or they could be of neural origin and reflect the frequency doubling caused by the summation of half-wave rectified neurophonic responses which are 180° out of phase due to the phase reversal of the stimulus. In order to determine if the response was of neural origin, we injected tetrodotoxin into scala tympani and found that it abolished the CAP, but it had virtually no effect on the large amplitude oscillations following the CAP. Thus, the oscillations presumably result from incomplete cancellation of the cochlear microphonic when stimulus phase is reversed 180° on alternate stimulus presentations.

The visual detection level of the CAP was assessed in 13 adult chickens in octave steps from 0.5 to 4 kHz. The mean thresholds plus and minus one standard deviation are shown in Fig. 2. The mean threshold decreased from approximately 42 dB SPL at 0.5 kHz to roughly 30 dB SPL at 1 and 2 kHz and then increased to 51 dB SPL at 4 kHz. The standard deviations ranged from a low of 3.3 dB at 2 kHz to 9.2 dB at 4 kHz.

Threshold

Cochlear ganglion neurons were encountered over a depth of 500–600 microns from the surface of the ganglion. Tuning curves were recorded from a total of 297 neurons from 14 animals in this study. Contact was lost with some of these neurons before the entire protocol was

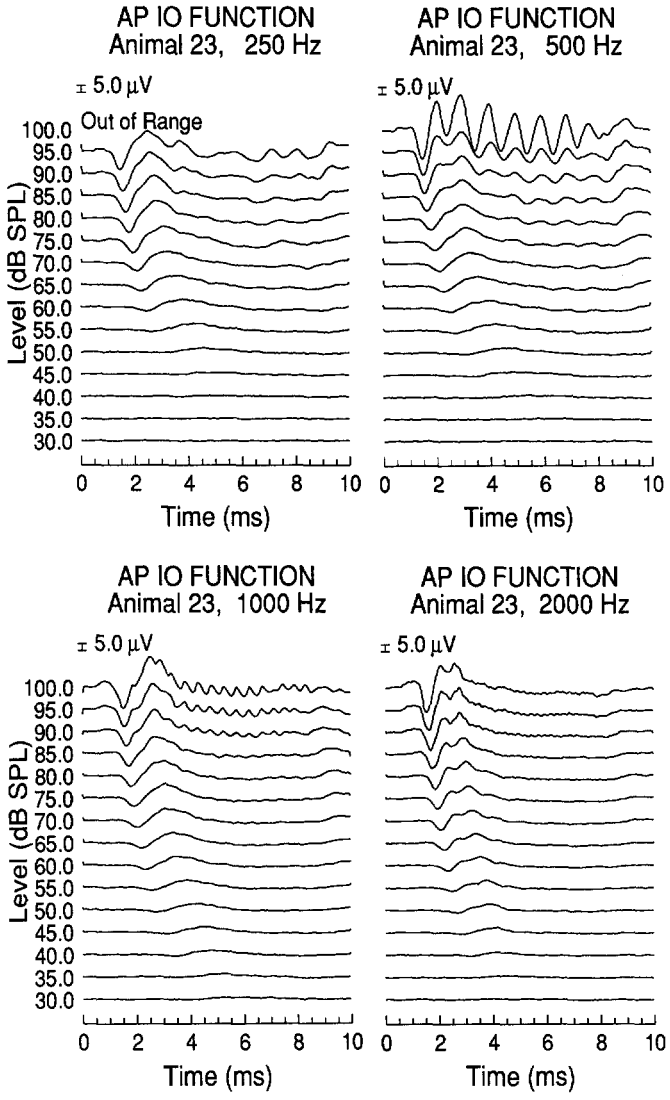

Fig. 1. Evoked responses recorded from the round window of a typical subject. The response is visible at 30–35 dB at 1000 Hz and 2000 Hz but not until 45–50 dB at 500 Hz and 250 Hz. Note the oscillations at higher stimulus levels in the 500 Hz and 1000 Hz tracings

completed; therefore, the number of units shown in subsequent analyses will vary somewhat. Figure 3 shows the threshold of each unit at its CF, i.e., the frequency at which threshold was lowest. For ease of comparison, the mean threshold of the compound action potential is also shown. Single unit CFs ranged from approximately 100 Hz to slightly more than 2000 Hz. Threshold at CF ranged from a high of 80 dB SPL near 100 Hz to a low of around 0 dB SPL between 500 and 1000 Hz. At any given CF, the range of thresholds is relatively large and at some frequencies the range exceeded 60 dB. In general, thresholds were lowest among units with CFs between 600 and 2000 Hz and gradually increased in units with progressively lower CFs. For any given CF, the threshold of the most sensitive units was typically 20–30 dB lower than the threshold of the CAP. In fact, the thresholds of most units lie below the mean compound action potential audiogram.

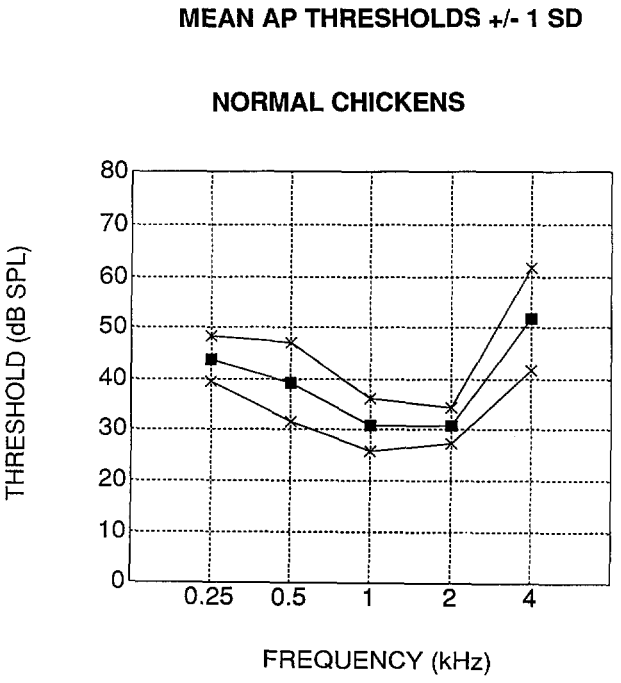

Fig. 2. CAP thresholds as a function of frequency averaged over 13 animals. Filled squares indicate means, X's indicate plus and minus one standard deviation. Testing was performed at octave frequencies from 250 Hz to 4 kHz

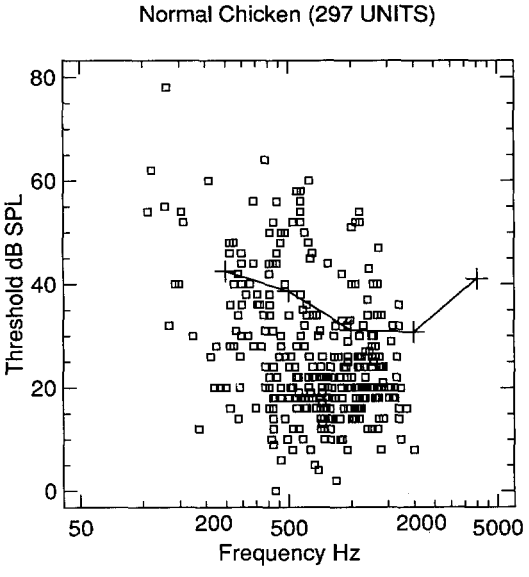

Fig. 3. Threshold for 297 units from chicken cochlear ganglion as a function of characteristic frequency. For comparison, mean CAP threshold for the 13 subjects is replotted from Fig. 2 by the +s connected with solid lines

Spontaneous discharge rate

The spontaneous discharge rate was measured from a total of 327 cochlear ganglion neurons. Figure 4 shows the distribution of spontaneous discharge rates for the sample of units in this study. Spontaneous rates ranged from essentially zero in a few units to slightly more than

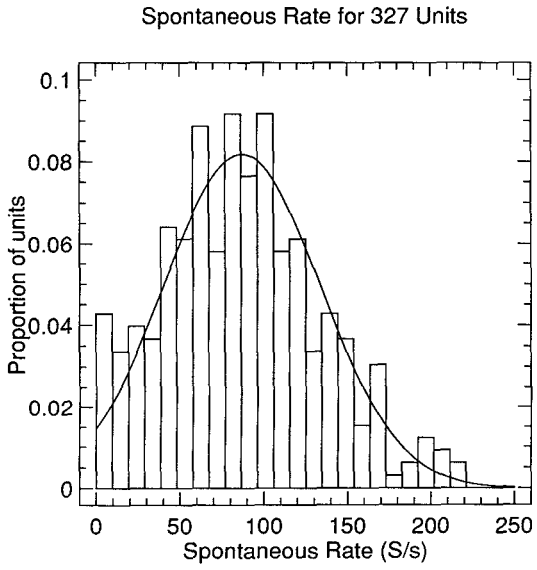

Fig. 4. Distribution of spontaneous firing rate for 327 cochlear ganglion units from 14 normal hearing chickens. The solid line represents a normal distribution with mean of 86 spikes/s and standard deviation of 49 spikes/s

200/s in others; however, the majority of units have spontaneous rates between 50 and 120 spikes/s. The distribution, for the most part, appears to be unimodal with no suggestion of other major peaks. Moreover, the distribution matches rather well with the solid line in Fig. 4, which represents a normal distribution with a mean of 86 and a standard deviation of 49.

Figure 5 shows 9 inter-spike interval histograms (bin width 0.1 ms) of spontaneous activity for units with CFs ranging from 252 Hz to 1099 Hz and spontaneous rates ranging from 36 to 191 spikes/s. Interspike interval histograms increase in CF from top to bottom in the figure. Within each row, spontaneous rate increases from left to right. While a detailed analysis has not been carried out, several trends are apparent in the data. First, the interspike interval histograms of moderate-to-high spontaneous rate units generally contained well defined peaks which decayed from the modal value in an exponential fashion. When multiple peaks were present in the histograms (middle-right columns), the time period (P) between peaks was approximately equal to the reciprocal of the unit's CF (P = 1/CF). The histograms from low spontaneous rate units (left column), by contrast, were relatively noisy due to the low number of spikes per bin which made it impossible to determine if peaks were also present in the histograms from low spontaneous rate units. Since most of our interspike interval histograms were constructed from a 10 s sample of spontaneous activity, the number of spike counts per bin was often too low to accurately characterize the histograms and to determine the existence of these preferred intervals. This causes the number of units with preferred intervals to be underestimated. However, it is clear that the majority of units in our sample do exhibit preferred time intervals. The second point to note is that the modal value of the histograms generally decreased as CF increased (middle-right columns) although the relationship between these two variables did not appear to be a particularly strong one.

Spontaneous rate and threshold

In the process of collecting the data it became apparent that the low spontaneous rate units tended to have high thresholds. In order to evaluate the relationship between threshold and spontaneous rate in more detail, it was necessary to control for the tendency towards lower thresholds at higher CF. In order to minimize this effect, spontaneous rate versus threshold plots were constructed for 4 discrete CF bands. As shown in Fig. 6, there is typically an inverse relationship between threshold and spontaneous rate, i.e., units with the lowest spontaneous rates typically have the highest thresholds. Regression lines were determined separately for each panel. The slopes for units with CF between 500 Hz and 1000 Hz (-0.16 ± 0.02 dB/S/s, $t(df = 134) = -8.25$, $P < 0.0001$) and for units with CF between 1000 Hz and 1500 Hz (-0.07 ± 0.02 dB/S/s, $t(df = 76) = -3.46$, $P < 0.001$) were significantly different from 0, while slopes for units with CF below 500 Hz and for units with threshold above 1500 Hz were not significantly different from 0. The regression accounted for a significant proportion of the variance in the two middle CF bands ($F(1/134) = 68.129$, $P < 0.0001$ and $F(1/76) = 11.935$, $P < 0.001$, respectively) but not for the units with CF less than 500 Hz ($F(1/91) < 1.0$) or for units with CF greater than 1500 Hz ($F(1/17) = 1.862$, $P > 0.10$). While there appears to be an inverse relationship between threshold and spontaneous rate in the lowest CF band, the correlation is obscured somewhat by the fact that the thresholds vary somewhat among units within this band. Slope and intercept for each panel are indicated in the panel.

Tuning curves

Figure 7 shows 9 different tuning curves obtained from units with CFs ranging from 287 Hz to 1696 Hz and having spontaneous rates ranging from 1 spike/s to 216 spikes/s. CF increases from top to bottom in the figure while spontaneous rate increases from left to right in each row. Several trends are apparent in the data. First, the tuning curves are quite sharply tuned particularly among units with CFs between 1–2 kHz. Second, for a particular CF range, units with lowest spontaneous rates appear to be more broadly tuned than those with the highest spontaneous rates. Third, the tuning curves are primarily V-shaped with little evidence of a broad, low-frequency tail. In fact, one striking aspect of the data is the steep slope of the tuning curve below CF, which in many cases appears to be equal to the high frequency slope. To illustrate this point, the low frequency slope and high frequency slope of the tuning curve were calculated between + 10 and + 30 dB re threshold at CF. The ratio of low frequency slope to high frequency slope was then

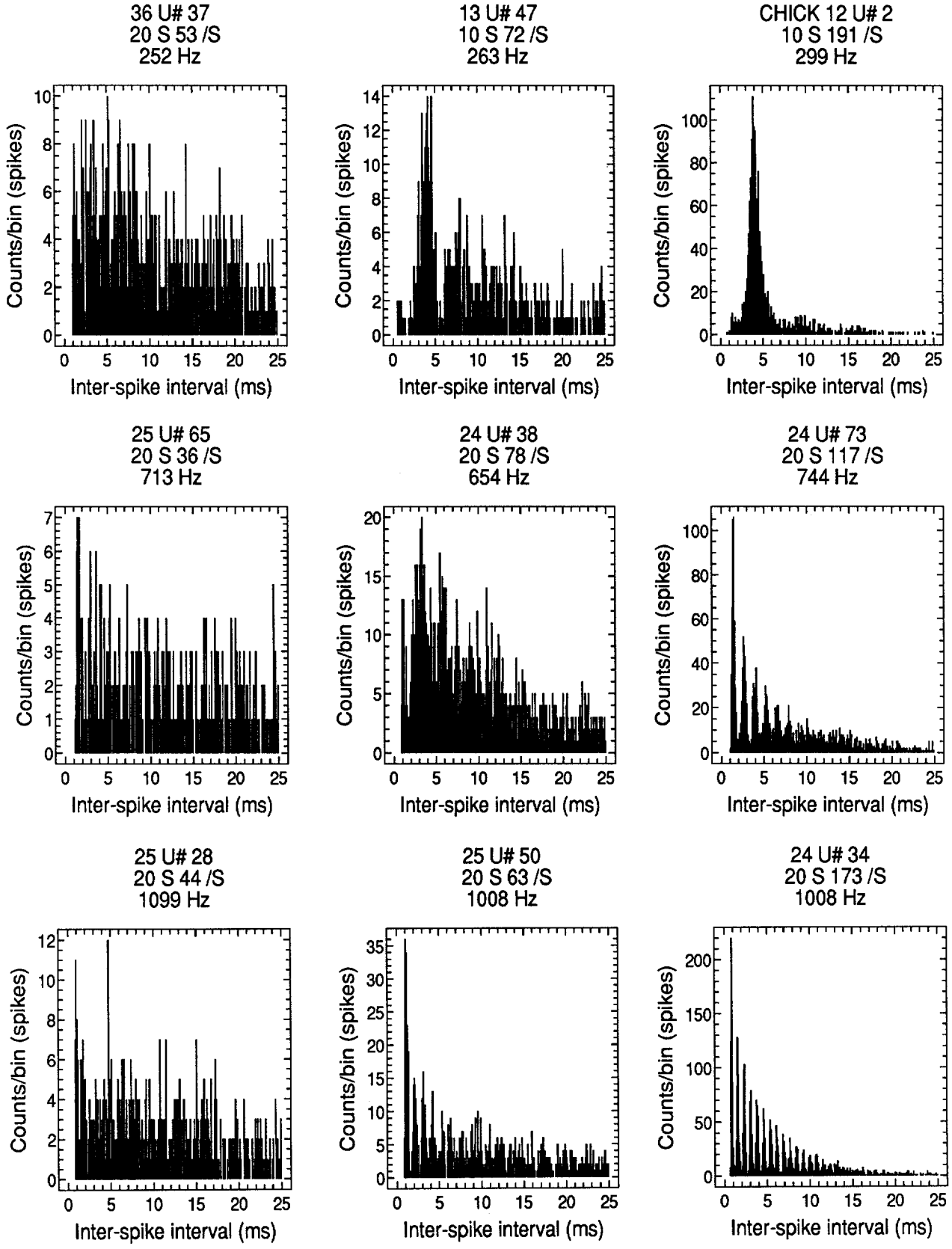

Fig. 5. Inter-spike interval histograms for spontaneous activity from 9 exemplary units from chicken cochlear ganglion. Bins are 0.1 ms. The figure is arranged with spontaneous rate increasing from left to right and CF increases from top to bottom. Note the multiple peaks, which are particularly prominent in the units with highest spontaneous rate

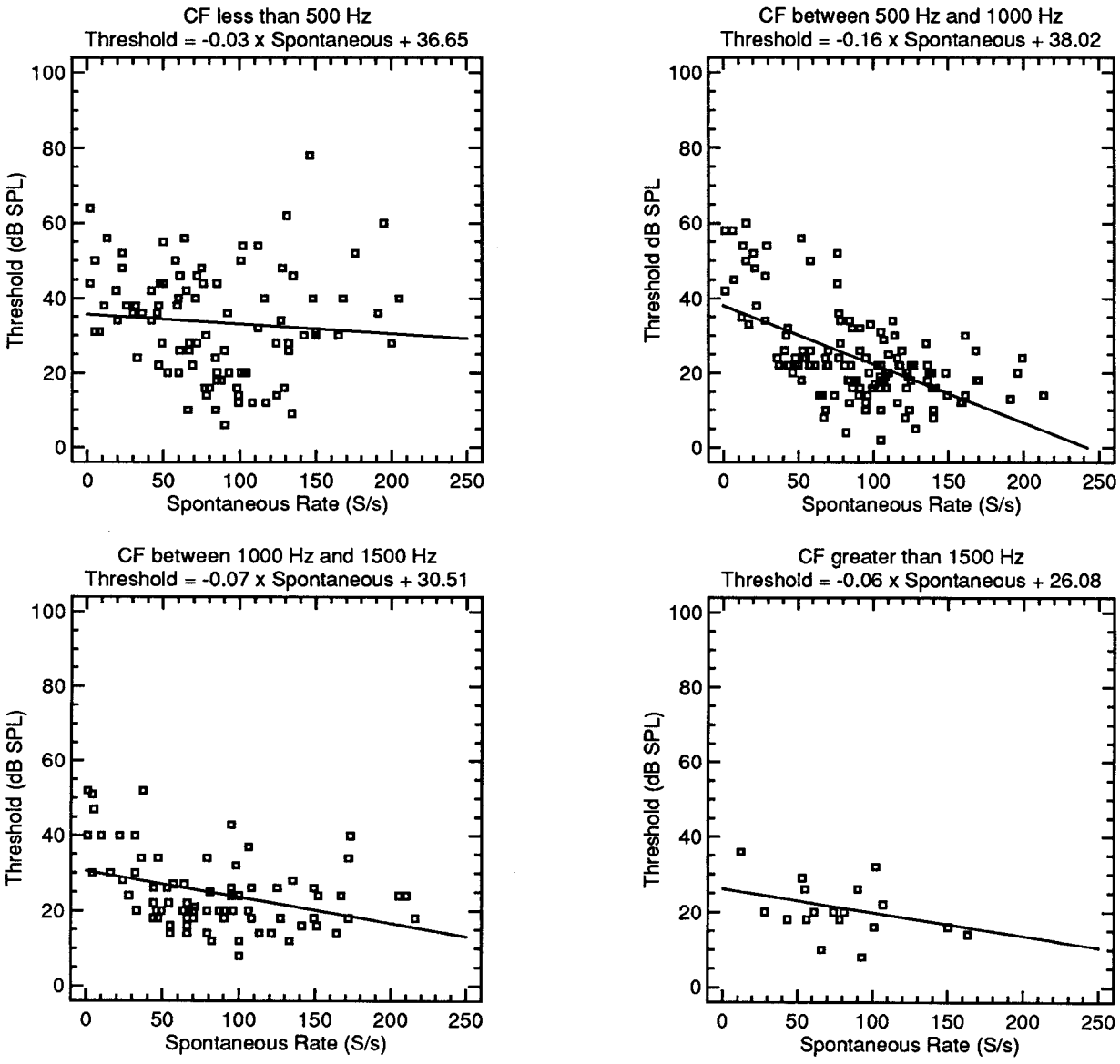

Fig. 6. Threshold as a function of spontaneous rate for units from chicken cochlear ganglion. Plots are divided into 4 CF regions to compensate for change in threshold with CF. There is generally an inverse relationship between CF and threshold, particularly for the 2 center CF bands. Lines are best-fitting linear relationship for each panel, with parameters indicated in the second line of the title of each panel. Slopes are significantly different from 0 for the middle two panels

plotted as a function of CF (Fig. 8). Most of the values tend to cluster around one with about the same number of units having values greater than or less than one.

The sharpness of the tuning curves was quantitatively assessed by determining the Q_{10dB} and Q_{30dB} values, i.e., the CF normalized by the bandwidth of the tuning curve at +10 dB or +30 dB above the threshold at CF respectively. Figure 9A shows the Q_{10dB} values and Fig. 9B shows the Q_{30dB} values for each unit plotted as a function of CF. The Q_{10dB} values show a fair amount of scatter with values ranging from 1 to 24; however, most of the values lie between 2 and 12. There is a slight tendency for the Q_{10dB} values to increase with CF. The Q_{30dB} values range from approximately 0.5 to 5.0 and show less scatter than the Q_{10dB} values. On average, the Q_{30dB} values show a gradual increase from approximately 0.5 at the low frequencies to approximately 3.0 among units with CFs between 1–2 kHz. For individual units, tuning assessed by Q_{30dB} was broader than tuning assessed by Q_{10dB}, as the ratio Q_{10dB} to Q_{30dB} had a mean of 4.52, which was significantly greater than 1.0 by t test ($t(df=296)=14.25$, $P<0.0001$).

Post-stimulus time histograms

Figure 10 shows a series of post-stimulus time histograms (bin width 1 ms) from 3 representative cochlear ganglion neurons using 50 ms tone bursts presented at the CF of unit. CF increases from the top to the bottom row in the figure and within each row, stimulus level increases from +5 dB to +40 dB relative to threshold. All 3 units fired

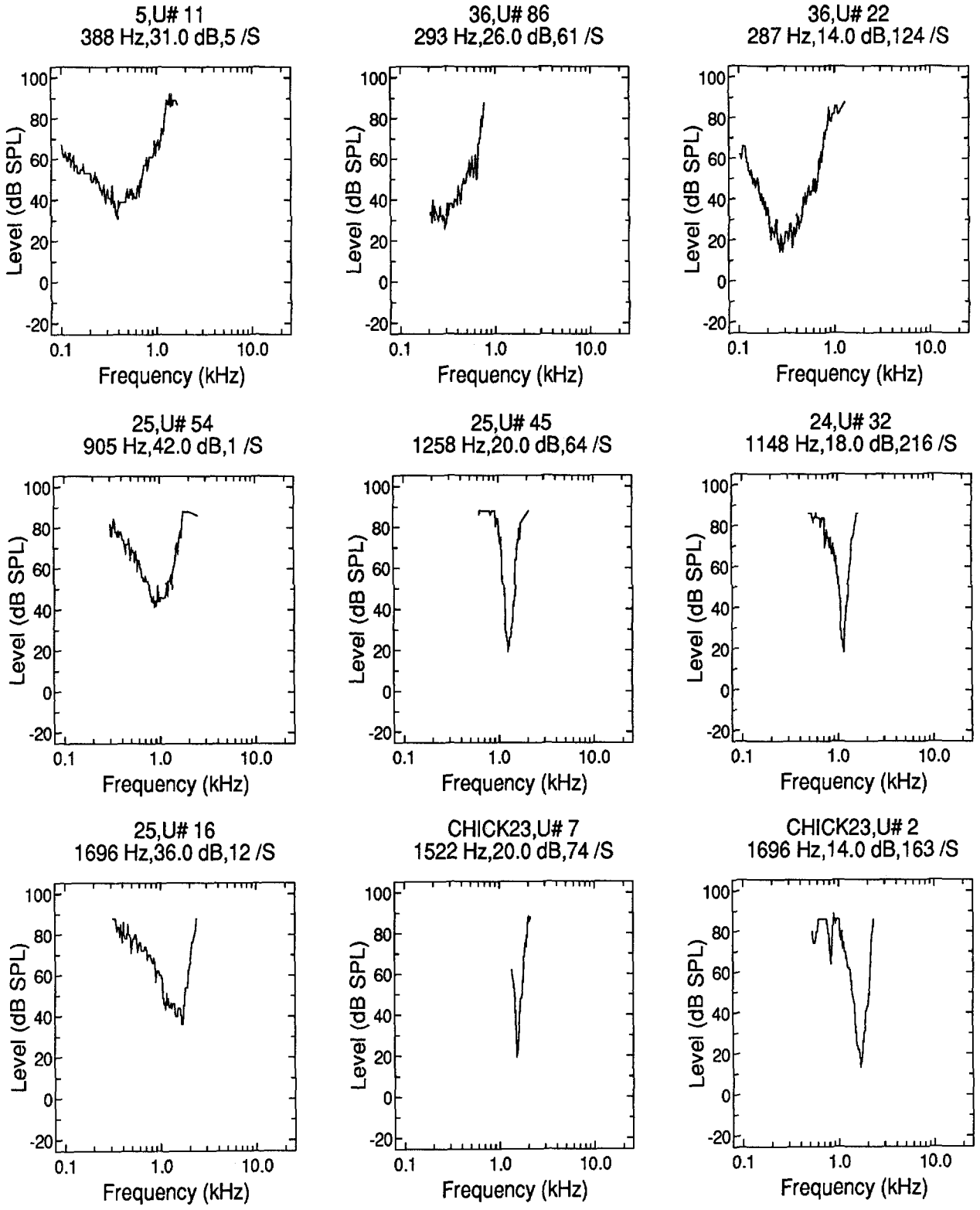

Fig. 7. Tuning curves from 9 cochlear ganglion units from normal hearing chickens. The plots are arranged so that spontaneous rate increases from left to right, while CF increases from top to bottom. The tuning curves are relatively sharp and generally have a symmetric (v) shape

in a sustained manner over the duration of the stimulus. The post-stimulus time histograms from the units with the two lowest CFs (top two rows Fig. 10) contain regularly spaced peaks due to the robust phase locking to CF tones of low frequency (Fig. 16). The overall envelopes of the post-stimulus time histograms from the units with the two lowest CFs are either rectangularly shaped or show only a slight-to-moderate sized peak at the onset

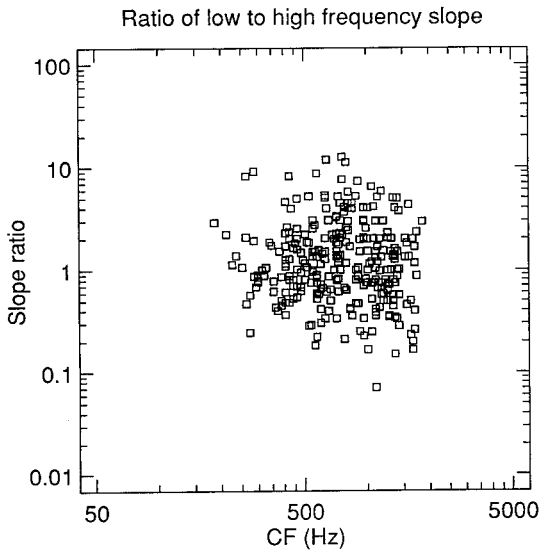

Fig. 8. Ratio of low frequency slope to high frequency slope between 10 dB and 30 dB above threshold for units from chicken cochlear ganglion. Values tend to cluster near 1, with about equal numbers above and below, and there is no apparent trend with CF

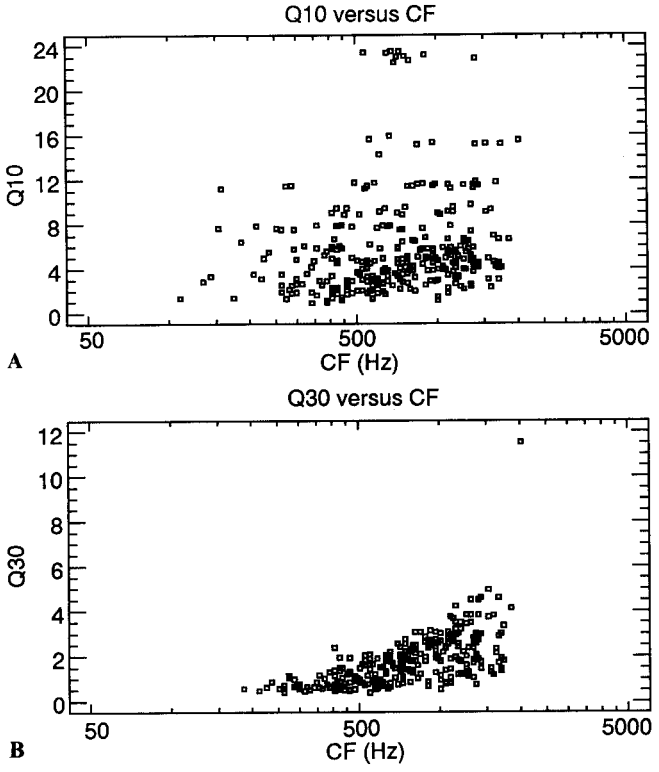

Fig. 9. Q_{10db} (**A**) and Q_{30db} (**B**) for units as a function of CF. Q is CF normalized to the bandwidth at the designated level above threshold. Q_{10} values are scattered, while Q_{30} values are more compact and show a slight tendency to increase with CF

of the stimulus followed by a very gradual decay over the duration of the stimulus. Compared to the two low CF units, the post-stimulus time histograms from the unit with the highest CF (bottom row Fig. 10) showed a more prominent peak near stimulus onset followed by a gradual decay in firing rate over the duration of the stimulus. In general, as stimulus level increased, the overall height of the histogram increased. Moreover, at the offset of the stimulus, the probability of firing showed an abrupt decrease followed by a gradual recovery of neural activity toward the spontaneous discharge rate.

All of the cochlear ganglion neurons responded in a sustained manner to acoustic stimuli presented at CF. However, on a few occasions, post-stimulus time histograms were collected using high-level tone bursts located near the high-frequency and low-frequency edges of the tuning curves. Under these conditions, the units tended to respond only near the onset and offset of the stimulus suggesting that the units were being activated by spectral splatter present at the onset and offset of the tone burst.

Discharge rate-level functions at CF

Discharge rate-level functions were measured at CF using 50 ms tone bursts presented at levels which typically spanned the range from −10 dB to 70 dB re the tuning curve threshold at CF. The discharge rate-level functions of most units increased monotonically with stimulus level over a 30–60 dB range after which the discharge rate saturated. For a small number of units, response rate declined by 10% or more of the maximum rate at the highest level collected. In all such cases, contact was lost with the unit at the next higher level, leading us to question whether the decline in rate was authentic, or due to loss of contact with the unit. There were no cases in which the rate declined from its maximum value over 2 or more levels. The dynamic range, which represents the dB range between threshold and the lowest level producing saturation firing rate, was evaluated in 121 cochlear ganglion neurons with CFs between 174 and 2017 Hz. As shown in Fig. 11, the dynamic range distribution is approximately normally distributed and has a mean of 41.8 dB and standard deviation of 8.49 dB. The distribution of saturation discharge rates for the sample of units was also normally distributed (Fig. 12). The saturation discharge rate ranged from 140 to 520 spikes/s with a mean of 327 and standard deviation of 83. There was no apparent relationship between the dynamic range and the saturation discharge rate. Both dynamic range and saturation discharge rate were positively correlated with spontaneous rate. As shown in Fig. 13, slope of the discharge rate-level function was negatively correlated with spontaneous rate ($r = -0.33$, $P < 0.01$). There was also no apparent relationship between the saturation discharge rate and CF or the dynamic range and CF.

Phase locking

The degree of phase locking seen in cochlear ganglion neurons was assessed by calculating the vector strength (Goldberg and Brown 1969). Since all of the cochlear ganglion neurons in this study had CFs below 2.5 kHz, they generally showed robust phase locking to tones

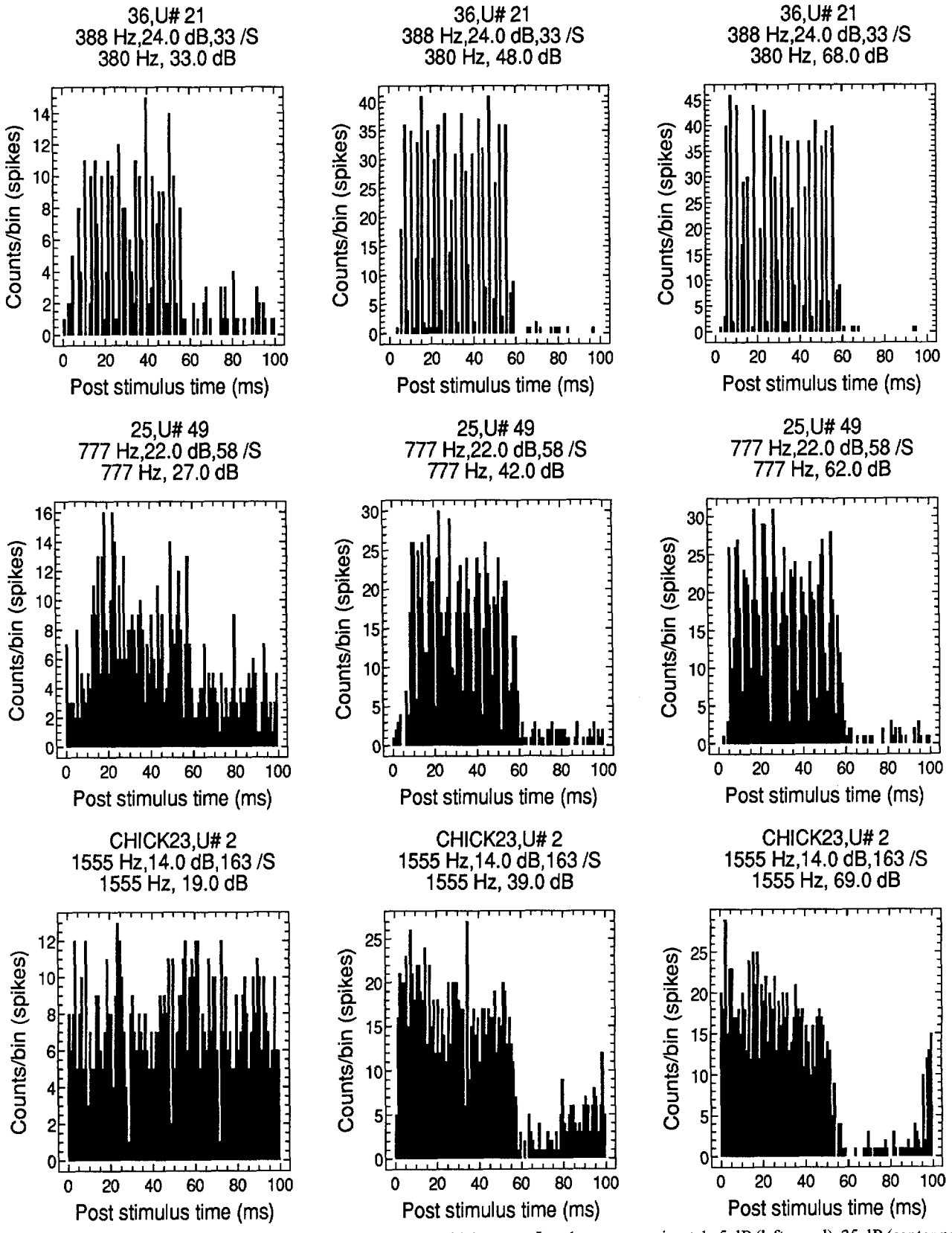

Fig. 10. Post stimulus time histograms for 3 units from chicken cochlear ganglion. CF increases from top to bottom of the figure. Levels are approximately 5 dB (left panel), 25 dB (center panel), and 40 dB (right panel) re threshold

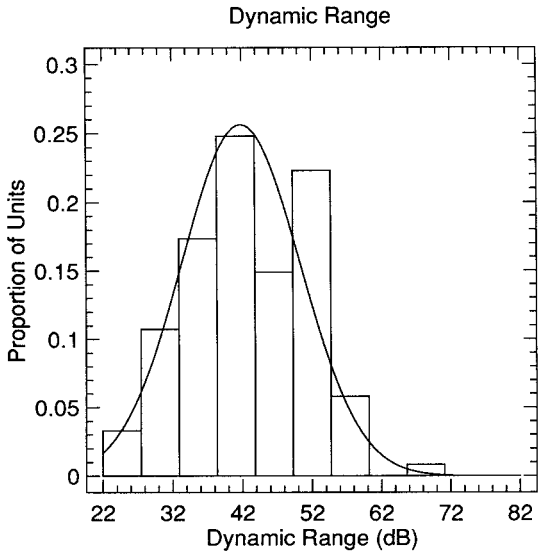

Fig. 11. Distribution of dynamic range for 121 units from chicken cochlear ganglion. The solid line represents a normal distribution with mean 41.8 dB and standard deviation 8.49 dB

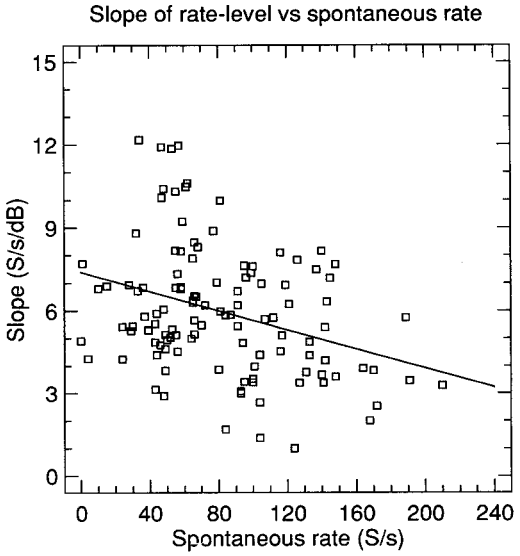

Fig. 13. Slope of rate versus level function as a function of spontaneous rate. Slope declines with spontaneous rate producing a negative correlation, $r = -0.33$, significant at $P < 0.01$

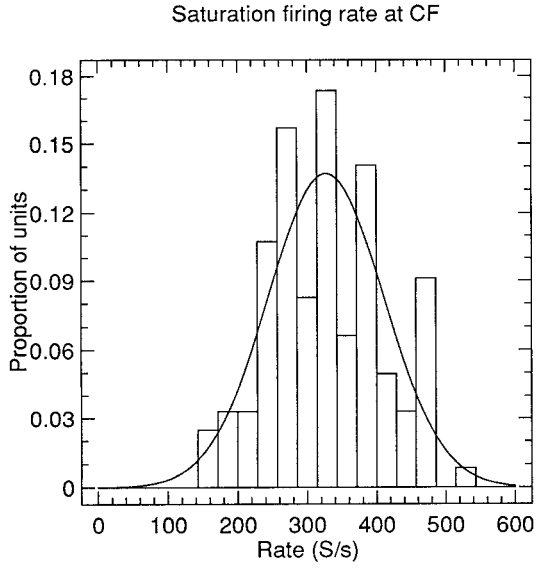

Fig. 12. Distribution of saturation firing rate for 121 units from chicken cochlear ganglion. The solid line represents a normal distribution with mean 327 spikes/s and standard deviation 83 spikes/s

presented at CF. Comparison of rate versus level and phase locking versus level for 9 units differing in CF and in spontaneous rate is presented in Fig. 14. As illustrated in Fig. 14, phase locking appeared within 5 dB of the rate threshold estimated from the tuning curve procedure; however, phase locking saturated before discharge rate saturation was reached. Thus, the dynamic range of phase locking was typically somewhat smaller than the dynamic range for firing rate. Once threshold was exceeded, most units exhibited fairly robust phase locking as illustrated in Fig. 15 which shows the distribution of vector strength values obtained with CF tones presented 20 dB above threshold. The distribution of vector strength values was essentially normally distributed with a mean of 0.665 and standard deviation of 0.102. Although phase locking was fairly robust for CF tones presented 20 dB above threshold, vector strength values showed a systematic decrease with increasing CF as illustrated by the scatterplot shown in Fig. 16. The best fitting line, with slope of -1.35×10^{-4} vector strength/Hz and intercept of 0.78 vector strength, accounts for 30.4% of the variance in vector strength. The fit to linear CF was slightly better than the fit to log CF.

Discussion

CAP

The CAP recorded from the round window has frequently been used to assess the functional integrity of the cochlea in mammals (Dallos et al. 1978), but only recently have data been reported for Leghorn chickens (Patuzzi and Bull 1991). Our CAP thresholds are slightly lower than those reported by Patuzzi and Bull (1991). In addition, our CAP audiogram shows a clear minimum between 1 and 2 kHz whereas Patuzzi and Bull (1991) reported that thresholds were relatively constant between 0.2 and 2 kHz. Our CAP thresholds are also in extremely good agreement with the evoked response thresholds from nucleus magnocellularis reported by McFadden and Saunders (1989). All 3 sets of data show that thresholds are lowest between 1 and 2 kHz. Thresholds gradually increase toward the low frequencies, but increase rapidly above 2 kHz. The CAP thresholds generally remained fairly stable over the recording session unless the preparation deteriorated, at which time the experiment was terminated.

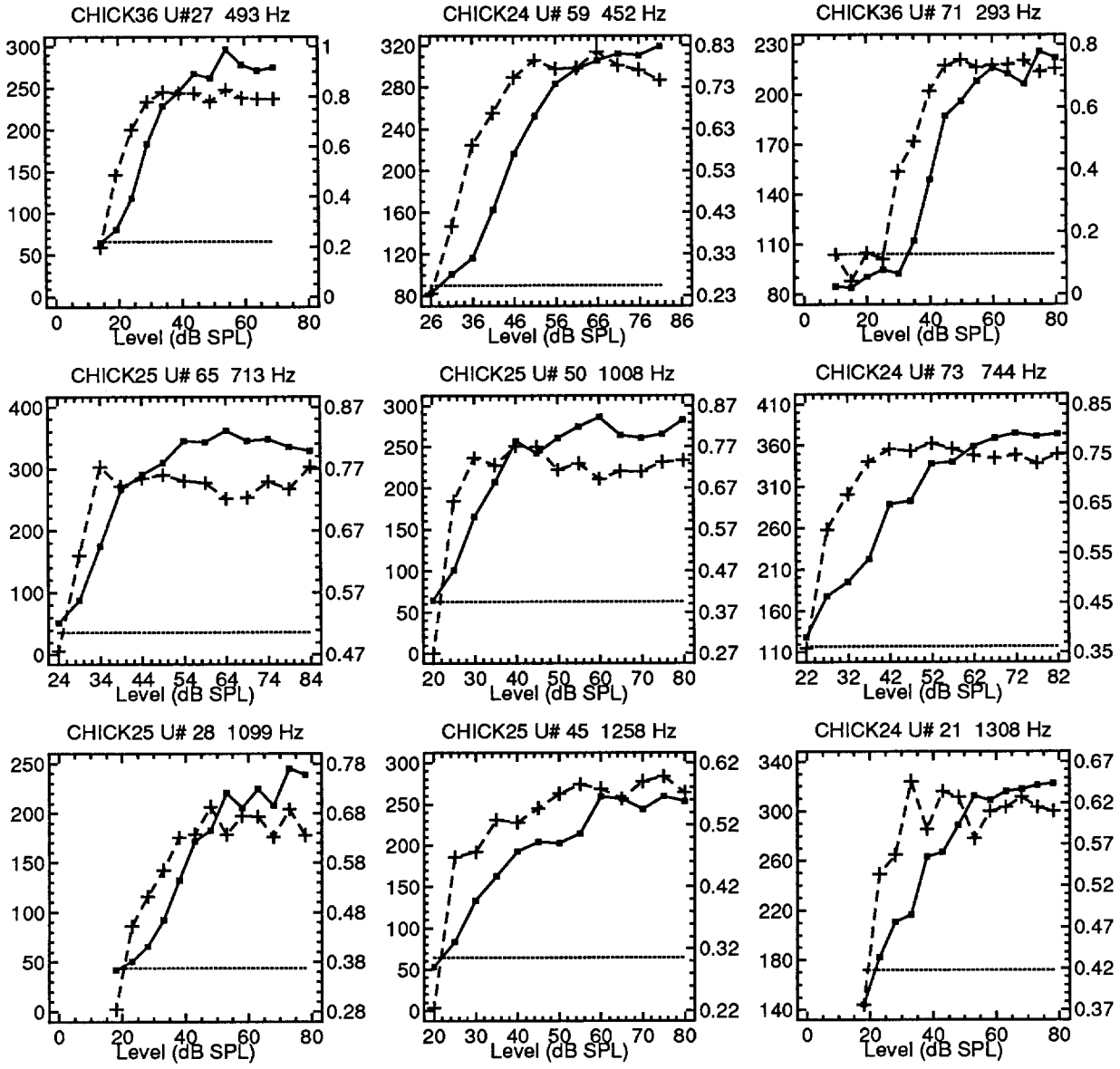

Fig. 14. Rate versus level (squares and solid line; left axis) and vector strength versus level (crosses and dashed line; right axis) for 9 units, showing features typical of the sample. The horizontal dotted line in each panel is at the spontaneous rate determined separately for the unit. Rate increases with level over approximately 40 dB before reaching a plateau. Vector strength increases with level starting at the same or slightly lower level and reaches a plateau at a slightly lower level than rate

Characteristic frequency

Although the CAP could be recorded at a moderate sound level at 4 kHz, we were unable to record from cochlear ganglion neurons with CFs much above 2 kHz in the present study. However, in one recent experiment, using the same procedure but a different preparation (2 months post-Kanamycin treatment), we were able to record from a few units with CFs in the range of 3–3.6 kHz. The range of CFs reported by Manley et al. (1987) using essentially the same surgical approach to the cochlear ganglion is quite similar to that reported here. By contrast, Warchol and Dallos (1990) were able to record from neurons in nucleus angularis with CFs as high as 4.8 kHz. It is possible that the paucity of high CF units encountered in this study is related to the use of pentobarbitone anesthesia as opposed to ketamine which was used by Warchol and Dallos (1990). To evaluate this possibility, we have used ketamine anesthesia in more recent studies, but have found essentially no difference in the range of CFs encountered with these two types of anesthetics. Thus, these results suggest that surgical approach used in this study is best suited to recording from units with moderate to low CFs in chickens. While the surgical procedure is relatively rapid and clearly less traumatic than approaching the auditory nerve intracranially, it does have several disadvantages as previously noted (Manley et al. 1985). First, the opening to scala tympani is closest to the basal end of the basilar papilla making this region more vulnerable to mechanical dam-

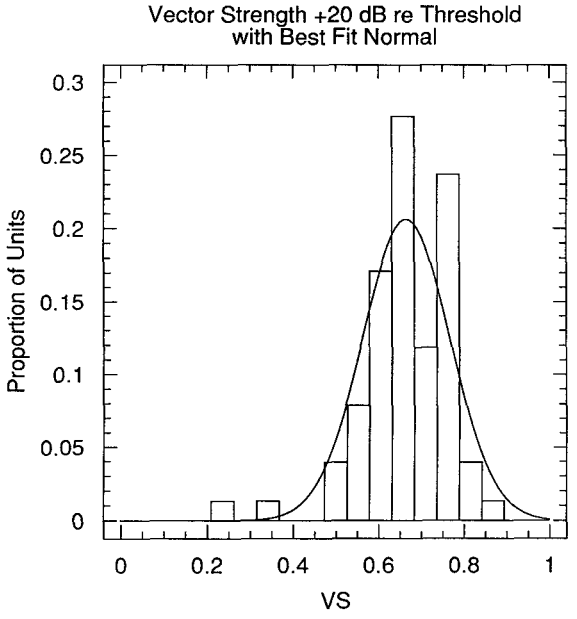

Fig. 15. Distribution of vector strength 20 dB above rate threshold as determined from the tuning curve, at CF. The solid line represents a normal distribution with mean 0.665 and standard deviation 0.102

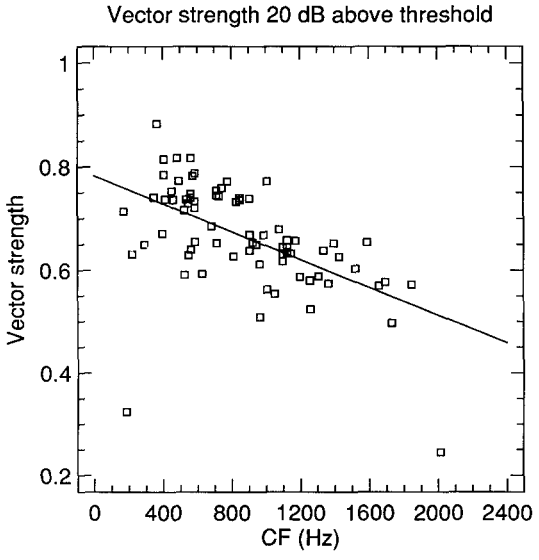

Fig. 16. Vector strength 20 dB above rate threshold at CF as determined from the tuning curve. Although vector strength is substantial for most units, there is a marked decline in vector strength with increasing CF. The regression line, with slope of -1.3×10^{-4} and intercept of 0.783, accounts for 30.44% of the variance

age. Second, fluid levels within scala tympani can drop unless the animal is given adequate bird Ringers' solution. Finally, it is difficult to sample high CF units with this approach.

Thresholds

The best single unit thresholds for a given CF were approximately 30–35 dB lower than the corresponding CAP threshold. In mammals, a difference of 15 to 25 dB between the CAP and the lowest unit thresholds would be more typical (Dallos et al. 1978). The CAP is believed to arise from the summed, synchronous response of many different neurons to the onset of the stimulus and for appropriately shaped tone bursts, the response is relatively frequency specific (Dallos et al. 1978). One factor that may give rise to a larger difference between the CAP and single unit thresholds in chickens is the degree of neural synchrony across units at stimulus onset. An informal comparison of post-stimulus time histograms from chickens and mammals suggests that the onset peak of the histograms is less pronounced in chickens. One characteristic of these neurons that could conceivably attenuate the amplitude of the onset peak is the relatively high spontaneous discharge rate which would tend to increase the probability of being refractory at stimulus onset, and thus reduce the degree of neural synchrony across the population of units. Many other factors could also be involved such as the number of active units at a given stimulus level, the rate of rise of excitatory post-synaptic potentials as well as differences in response latency between units.

At any particular CF, the range of thresholds was quite large in the chicken, on the order of 60 dB. Moreover, the units with the lowest spontaneous rates generally had the highest thresholds. It is highly unlikely that the broad range of thresholds was due to some form of pathology since the high and low threshold units were encountered in random order within the same animal. Moreover, a wide range of thresholds and an inverse relationship between threshold and spontaneous rate has also been reported in starlings (Manley et al. 1985), several species of mammals (Liberman 1978; Salvi et al. 1982) and in the caiman (Klinke and Pause 1980). Thus, the results from the chicken are consistent with the results of a number of different species.

The thresholds of our most sensitive cochlear ganglion neurons were somewhat lower than the most sensitive units seen in either nucleus angularis or nucleus magnocellularis of the chicken (Warchol and Dallos 1990). One factor that may partially account for these differences is the criterion used to obtain the tuning curves. The criterion used in our study was a 1 spike difference (20 spikes/s) between the tone and no-tone counting intervals (50 ms) versus a two spike difference (40 spikes/s) employed by Warchol and Dallos. Assuming a discharge rate-level function slope of 2–3 spike/s/dB for our low-threshold, high spontaneous rate units (Fig. 13), one would predict a threshold increase of between 7 and 10 dB by changing our threshold criterion from 1 to 2 spikes. Thus, increasing our threshold criterion would lead to better agreement between the thresholds of units in the cochlear nucleus and cochlear ganglion. The range of thresholds at a given CF is also different for units in the cochlear nucleus and cochlear ganglion. The range of

thresholds in the cochlear ganglion is on the order of 40–60 dB; this is similar to the range of thresholds seen in nucleus magnocellularis (50 dB), but larger than the range of thresholds seen in nucleus angularis (30 dB).

Spontaneous activity

The mean spontaneous discharge rate in the chicken was 86 spikes/s. This value is similar to that seen in pigeons and blackbirds (Sachs et al. 1980), but is considerably higher than the 30 spikes/s reported for cat (Sachs et al. 1974) or the 61 spikes/s reported for guinea pig (Manley and Robertson 1976). Sachs et al. (1974) suggested that birds have higher spontaneous rates than mammals because of their higher body temperature and metabolism. However, this explanation is difficult to reconcile with the fact that the spontaneous rate (45 spikes/s) in at least one species of bird, the starlings, is similar to that seen in mammals (Manley et al. 1985). It is unclear why starlings have such low spontaneous rates compared to other birds; however, it is unlikely to be due to procedural differences since our recording methods are essentially the same as those used by Manley et al. (1985).

Although different rates of spontaneous activity have been observed among avians, all appear to have unimodal spontaneous rate distributions. By contrast, the spontaneous rate distributions in mammals are typically bimodal with one peak near zero, a gap in the distribution near 20 spikes/s and a second peak around 40–60 spikes/s (Liberman 1978; Salvi et al. 1983). A bimodal distribution has also been seen in caiman (Klinke and Pause 1980). It has been suggested (Geisler 1981) that the bimodal distribution in mammals may result from having afferent fibers which differ in their sensitivity to the release of neurotransmitter packages from hair cells. Electron microscopic studies in the cat have revealed two classes of radial afferent fibers which may form the basis for this bimodal distribution (Liberman 1980). Thick fibers, which contain numerous mitochondria have been associated with high spontaneous rate units (>18 spikes/s). By contrast, thin fibers, which contain few mitochondria and which are sometimes associated with complex synapses, have been linked to low and medium spontaneous rate units (≤ 18 spikes/s). Since the distribution of spontaneous rates in birds appears to be unimodal, one might predict that the afferent fibers and associated synapses in birds are relatively homogeneous compared to those in mammals.

While the distribution of spontaneous rates in cochlear ganglion neurons is unimodal, the distributions of spontaneous rates in the cochlear nuclei are segregated into two groups based on recording location; neurons in nucleus angularis have low spontaneous rates (25 spikes/s) whereas those in nucleus magnocellularis have high spontaneous rates (94 spikes/s). It is conceivable that neurons in nucleus angularis receive inputs primarily from cochlear ganglion neurons with low spontaneous rates whereas neurons in nucleus magnocellularis might receive inputs primarily from cochlear ganglion neurons with high spontaneous rates. If this were the case, then one would expect that the thresholds of units in nucleus angularis would be lower than those in nucleus magnocellularis; however, the reverse appears to be true (Warchol and Dallos 1990). This would seem to suggest that the spontaneous rates in nucleus angularis and nucleus magnocellularis are based on the membrane properties of these cells and/or their synaptic arrangements.

Preferred intervals in the interspike interval histograms have been observed in primary auditory neurons in the turtle (Crawford and Fettiplace 1980), tokay gecko and starlings (Manley 1979; Manley et al. 1985). Manley has suggested that the preferred intervals, and the correlation between the modal interval of spontaneous activity and CF is indicative of a resonance mechanism within individual avian hair cells similar to that reported in turtles (Crawford and Fettiplace 1980). Recently, damped voltage oscillations, which depend on calcium-activated potassium currents, have been observed in tall hair cells isolated from the chick cochlea (Fuchs et al. 1988; Murrow and Fuchs 1989). The frequency of the oscillations increased in cells isolated from progressively more basal regions of the cochlea and when correction was made for the effects of temperature (Schermuly and Klinke 1985), the frequency of the oscillations corresponded to the vibration frequency for basilar membrane motion (von Békésy 1960) and the frequency-place map of the chick cochlea (Manley et al. 1987). This electrical resonance is believed to play an important role in determining the frequency selectivity of the cell and in generating the preferred intervals in the interspike interval histograms. While there is convincing evidence for electrical resonance in tall hair cells studied in vitro, any interpretation of the present data must be tempered by the absence of any electrical resonance seen in short hair cells recorded in vivo (Patuzzi and Bull 1991). However, this may not be a critical issue since most cochlear ganglion cells innervate tall hair cells whereas relatively few contact short hair cells (von Düring et al. 1985; Singer et al. 1989).

Tuning

As noted earlier, most of the tuning curves have a generally symmetric appearance, without a distinct low frequency tail which is typical of the tuning curves in mammals. As noted earlier, the low frequency slopes of chicken tuning curves were quite steep in agreement with data for starlings (Manley et al. 1985). In our sample of units, the slope of the low frequency side of the tuning curve was nearly the same as the slope of the high frequency side across CF. However, in starlings, the low frequency slope is somewhat steeper than the high frequency slope in low CF units whereas in units with CFs above 1600 Hz the reverse is true (Manley et al. 1985). Since our sample contains relatively few units with CFs above 1600 Hz, it is unclear if the ratio of high frequency to low frequency slope increases at higher frequencies. However, in nucleus angularis and nucleus magnocellularis, the high frequency slope of the tuning curves increases with CF

particularly above 1500 Hz, whereas the low frequency slope remains fairly constant across CF (Warchol and Dallos 1990). Thus, it is likely that a similar trend is present in high CF units from the cochlear ganglion.

Response types

Three different types of discharge patterns, primarylike, chopper and on, have been described in the two divisions of the cochlear nucleus of the chicken (Warchol and Dallos 1990). Thus, it may be useful to compare the post-stimulus time histograms of units in the cochlear ganglion with those in the cochlear nucleus to determine the extent of neural recoding that occurs between these two nuclei. All of the units in nucleus magnocellularis and 40% of the units in nucleus angularis had primarylike response patterns. The post-stimulus time histograms of primarylike units, by definition, should be similar to those of our cochlear ganglion neurons. The 3 primarylike histograms shown in the study of Warchol and Dallos (1990) all had CFs of 1500 Hz or greater. All of their primarylike histograms had a peak near stimulus onset followed by gradual decay to a plateau level 30 to 40 ms after stimulus onset. The post-stimulus time histograms of the one high-CF cochlear ganglion neuron shown in Fig. 10 are similar to those of the primarylike units in the cochlear nucleus. By contrast, the post-stimulus time histograms of low-CF cochlear ganglion neurons (Fig. 10 top and middle row) seldom contained a distinct peak at stimulus onset and thus differ from high-CF units in both the cochlear ganglion and cochlear nucleus. Since Warchol and Dallos (1990) did not present any data from units with CFs below 1500 Hz, we do not know if the histograms of low-CF primarylike units in the cochlear nucleus differ from those in the cochlear ganglion. However, in the auditory nerve of mammals, the size of the onset peak of the post-stimulus time histogram decreases as CF decreases. In fact, in some low-CF units, the onset peak is completely absent (Rhode and Smith 1986). Thus, the trends observed in the cochlear ganglion of the chicken appear to be consistent with those in mammals.

None of post-stimulus time histograms from cochlear ganglion were of the on or chopper type when CF tones were used to drive the unit. Thus, the on and chopper histograms seen in nucleus angularis of the chicken must arise from neural recoding within this nucleus. However, on a number of occasions, we have observed onset and offset responses from cochlear ganglion neurons when high level tone bursts were presented near the high or low frequency edge of the units' excitatory response area. These onset and offset responses presumably arise from spectral splatter associated with onset and offset of the stimulus as has been noted in the cat (Rhode and Smith 1986) and starling (Manley et al. 1985).

Dynamic range

As in other avian ears, the discharge rate-level functions of cochlear ganglion neurons in the chicken were monotonic. The dynamic range of units in the cochlear ganglion of the chicken appears to be slightly higher than that typically seen in mammals, and is substantially higher than the mean dynamic range of 25 dB (range 25 to 50) reported by Manley et al. (1985) for the starling. The mean of 44 dB for nucleus angularis and 38 dB for nucleus magnocellularis in chicken (Warchol and Dallos 1990) is quite close to the mean of 42 dB seen in this study. In contrast to cells in the starling cochlear ganglion and cells in nucleus angularis and nucleus magnocellularis in the chicken, there was no correlation between dynamic range and asymptotic rate in the present data, although both asymptotic rate and dynamic range correlated with spontaneous rate. The slopes of the discharge rate-level functions in chicken cochlear ganglion are negatively correlated with spontaneous rate, and may be more variable than slopes of rate versus level functions in starling cochlear ganglion or chicken cochlear nucleus. The negative correlation between spontaneous rate and slope of the rate versus level function in the present data contrasts with the finding from the cat (Liberman 1988), where low spontaneous rate units have the most gradual slopes. It should be noted, however, that chicken cochlear ganglion appears to be a single population in spontaneous rate, while cat afferent fibers can be divided into classes based on spontaneous rate. The negative correlation between slope and spontaneous rate in the chicken is a continuous relationship within one class, while the relationship noted by Liberman (1988) is one between classes.

Phase-locking

Virtually all of the cochlear ganglion neurons in our sample phase-locked robustly to stimuli presented 20 dB above the threshold at CF. Although the degree of phase locking declined with increasing CF, there was still substantial phase-locking among units with CFs up to 2 kHz. Since our sample of units was restricted primarily to those below 2 kHz, we do not know what the upper frequency limit of phase-locking is in the cochlear ganglion. Warchol and Dallos (1990) reported that units in nucleus magnocellularis exhibited significant phase locking (defined as a vector strength exceeding 0.2) up to approximately 2 kHz whereas units in nucleus angularis, most of which are classified as choppers, showed little phase-locking above 1 kHz. Examination of our phase-locking data between 1 and 2 kHz indicates that nearly all cochlear ganglion neurons have vector strength values greater than 0.5 whereas all of the neurons in nucleus magnocellularis have vector strength values less than 0.5. Visual inspection of the data between 1 and 2 kHz suggests that the vector strength values of cochlear ganglion neurons are approximately 0.25 greater than those in nucleus magnocellularis; this difference is similar to that seen in the redwing blackbird (Sachs et al. 1980). Moreover, in mammals, the vector strength values in the auditory nerve are 0.1–0.2 greater than those in the cochlear nucleus at a given frequency (Rhode and Smith 1986; Kettner et al. 1985).

Warchol and Dallos (1990) suggested that phase-locking might exist well beyond 2 kHz in cochlear ganglion neurons. Visual extrapolation of our phase-locking data (Fig. 16) suggests that significant phase-locking may persist up to at least 4–5 kHz in chicken cochlear ganglion neurons. This value is comparable to that reported for the redwing blackbird (Sachs et al. 1980); however, it is nearly an octave less than the upper limit of phase-locking reported for neurons in the cochlear nucleus of the barn owl (Sullivan and Konishi 1984).

Acknowledgements. Research supported by the Deafness Research Foundation and NSF (BNS9007822).

References

Békésy G von (1960) Experiments in hearing. McGraw-Hill, New York, pp 504–506

Corwin JT, Cotanche DA (1988) Regeneration of sensory hair cells after acoustic trauma. Science 240:1772–1774

Crawford AC, Fettiplace RR (1980) The frequency selectivity of auditory nerve fibers and hair cells in the cochlea of the turtle. J Physiol 306:79–125

Dallos P, Harris DM, Ozdamar O, Ryan A (1978) Behavioral, compound action potential and single unit thresholds: relationship in normal and abnormal ears. J Acoust Soc Am 64:151–157

Düring M von, Andres KH, Simon K (1985) The comparative anatomy of the basilar papillae in birds. Fortschr Zool 30:681–685

Fermin CD, Cohen GM (1984) Developmental gradients in the embryonic chick's basilar papilla. Acta Otolaryngol (Stockh) 97:39–51

Fuchs PA, Nagai T, Evans MG (1988) Electrical tuning in hair cells isolated from the chick cochlea. J Neurosci 8:2460–2467

Geisler CD (1981) A model for discharge patterns of primary auditory-nerve fibers. Brain Res 212:198–201

Goldberg JM, Brown PB (1969) Response of binaural neurons of dog superior olivary complex to dichotic tonal stimuli: some physiological mechanisms of sound localization. J Neurophysiol 32:613–636

Gray L (1990) Development of temporal integration in newborn chickens. Hearing Res 45:169–178

Gray L, Rubel EW (1985a) Development of absolute thresholds in chickens. J Acoust Soc Am 77:1162–1172

Gray L, Rubel EW (1985b) Development of auditory thresholds and frequency difference limens in chickens. In: Gottlieb G, Drasnegor NA (eds) Measurement of audition and vision in the first year of postnatal life: a methodological overview. Ablex, Norwood, pp 145–165

Jhavari S, Morest DK (1982) Neural architecture in nucleus magnocellularis of chicken auditory system with observations on nucleus laminaris: a light and electron microscope study. Neurosci 7:809–836

Kettner RE, Feng J-Z, Brugge JF (1985) Postnatal development of phase-locking response to low frequency tones of auditory nerve fibers in cat. J Neurosci 5:275–283

Klinke R, Pause M (1980) Discharge properties of primary auditory fibers in *Caiman crocodilus*; comparisons and contrasts to the mammalian auditory nerve. Exp Brain Res 38:137–150

Liberman MC (1978) Auditory-nerve response from cats raised in a low-noise chamber. J Acoust Soc Am 63:442–455

Liberman MC (1980) Morphological differences among radial afferent fibers in the cat cochlea: an electron-microscopic study of serial sections. Hearing Res 3:45–63

Liberman MC (1988) Physiology of cochlear efferent and afferent neurons: direct comparisons in the same animal. Hearing Res 34:179–192

Manley GA (1979) Preferred intervals in the spontaneous activity of primary auditory neurones. Naturwissenschaften 66:582

Manley GA, Robertson D (1976) Analysis of spontaneous activity of auditory neurones in the spiral ganglion of the guinea-pig cochlea. J Physiol 258:323–336

Manley GA, Gleich O, Leppelsack H-J, Oeckinghaus H (1985) Activity patterns of cochlear ganglion neurones in the starling. J Comp Physiol A 157:161–181

Manley GA, Brix J, Kaiser A (1987) Developmental stability of the tonotopic organization of the chick's basilar papilla. Science 237:655–656

McFadden EA, Saunders JC (1989) Recovery of function following intense sound exposure in the neonatal chick. Hearing Res 41:205–215

Murrow BW, Fuchs PA (1989) Electrical membrane properties of short hair cells from the chick's cochlea. Abstr Assoc Res Otolaryngol, St. Petersburg, Florida, Feb. 5–9, 136

Patuzzi RB, Bull CL (1991) Electrical responses from the chicken basilar papilla. Hearing Res 53:57–77

Rhode WS , Smith PH (1986) Encoding timing and intensity in the ventral cochlear nucleus of the cat. J Neurophysiol 56:261–286

Rubel EW, Parks TN (1975) Organization and development of brain stem auditory nuclei of the chicken: Tonotopic organization of N. magnocellularis and N. laminaris. J Comp Neurol 164:411–434

Rubel EW, Lippe WR, Ryals BM (1984) Development of the place principle. Ann Otol Rhinol Laryngol 93:609–615

Ryals BM, Rubel EW (1987) Hair cell regeneration after acoustic trauma in adult *Coturnix Quail*. Science 240:1774–1776

Sachs MB, Young ED, Lewis RH (1974) Discharge patterns of single fibers in the pigeon auditory nerve. Brain Res 70:431–447

Sachs MB, Woolf NK, Sinnott JM (1980) Response properties of neurones in the avian auditory system: comparisons with mammalian homologues and consideration of the neural encoding of complex stimuli. In: Popper AN, Fay RR (eds) Comparative studies of hearing in vertebrates. Springer, Berlin Heidelberg New York, pp 323–353

Salvi RJ, Perry J, Hamernik RP, Henderson D (1982) Relationships between cochlear pathologies and auditory nerve and behavioral responses following acoustic trauma. In: Hamernik RP, Henderson D, Salvi RJ (eds) New perspectives on noise-induced hearing loss. Raven Press, New York, pp 165–188

Salvi RJ, Henderson D, Hamernik RP (1983) Physiological basis of sensorineural hearing loss. In: Tobias J, Schubert E (eds) Hearing research and theory, Vol. 2. Academic Press, New York, pp 173–231

Saunders JC, Coles RB, Gates GR (1973) The development of auditory evoked responses in the cochlea and cochlear nuclei of the chick. Brain Res 63:59–74

Saunders JC, Tilney LG (1982) Species differences in susceptibility to noise exposure. In: Hamernik RP, Henderson D, Salvi RJ (eds) New perspectives on noise-induced hearing loss. Raven Press, N.Y., pp 229–248

Schermuly L, Klinke R (1985) Change of characteristic frequency of pigeon primary auditory afferents with temperature. J Comp Physiol A 156:209–211

Singer I, Fischer FP, Manley GA (1989) Hair-cell innervation in the basilar papilla in the European Starling *(Sturnus vulgaris)*. Abstr. 26th Workshop Inner Ear Biology, p 60

Sullivan WE, Konishi M (1984) Segregation of stimulus phase and intensity coding in the cochlear nucleus of the barn owl. J Neurosci 4:1787–1799

Tilney MS, Tilney LG, DeRosier DJ (1987) The distribution of hair cell bundle lengths and orientation suggests an unexpected pattern of hair cell stimulation in the chick cochlea. Hearing Res 25:141–151

Warchol ME, Dallos P (1990) Neural coding in the chick cochlear nucleus. J Comp Physiol A 166:721–734